

HIGH ENERGY NEUTRINO PHYSICS ($E_\nu > 20$ BeV)
AND THE CONSTRAINTS PLACED ON THE DETECTORS

M. L. Stevenson
Lawrence Radiation Laboratory

ABSTRACT

Two classes of high-energy neutrino experiments were considered: W production and the measurement of total cross section as a function of energy and momentum transfer.

The first experiment requires that converting material be placed primarily downstream to detect any π^0 or neutron decay fragments of the W which carries off most of the incident neutrino's momentum. The second experiment requires both downstream converter and transverse converter.

As a possible detector the BNL 25-foot bubble chamber was considered with a track-sensitive target cylinder of H_2 or D_2 placed in a 30% neon- H_2 mixture. The effective volume of H_2 and D_2 for the various experiments is summarized in graphical form. Generally the effective volume is less than 10 m^3 when one or more π^0 's are involved in the experiment. When a neutron is involved, the effective volume is less than 8 m^3 .

If the 25-foot chamber is changed from football shape to a basketball shape (23-foot diameter), a factor of \approx four is gained in the effective volume.

Generally, for neutrino physics, it is more important to measure curvature than angles. Therefore, the magnetic field should be kept as high as possible.

I. INTRODUCTION

The purpose of this note is to examine two possible experiments that utilize the highest energy neutrinos available in the neutrino beam. The primary aim is to determine the general detector configuration necessary to do these experiments.

A. Intermediate Vector Meson, (W)

Present experimental searches for the meson responsible for the weak interactions have failed to find evidence for such a meson with mass less than 2 BeV. The continuation of the search will be made at NAL with both counter-spark chamber systems and with bubble chambers. Whereas past studies have concentrated on the leptonic decay modes of the W, the considerations here will be more heavily weighted to the hadronic modes.

B. Total Neutrino Cross Section for all Channels

The present experimental data indicate that the total cross section is rising linearly with the laboratory neutrino energy. The fact that there will be many more particles in the final state will make the ambiguity problem greater and may introduce greater fractional uncertainties into the determination of the energy of the neutrino that produced the determination of the energy of the neutrino that produced the interaction. This in turn can result in a large error in the cross section.

II. W MESONS

Figure 1a displays the role the W is presumed to play in semi-leptonic decay and at the same time summarizes some of its possible decay modes. H and H' are the initial and final hadrons of the hadronic current, and l and l' are the corresponding elements of the leptonic current. If a W is produced (for example via the diagram of Fig. 1b) we know that it will decay semi-weakly via the modes,

$$W \rightarrow \bar{l} l' \quad (1)$$

and

$$W \rightarrow \bar{H} H' . \quad (2)$$

A. Leptonic Decay Modes

Schemes for detecting the leptonic mode (1) have been discussed in previous studies. Most of these schemes detect μ^\pm pairs and attempt to demonstrate that these pairs do not behave like those that would be generated by electromagnetic interactions. For example, Mel Schwartz³ has proposed an experiment in which the W is produced coherently in a 30-ton uranium target. The momentum of both muons is measured by spark chambers placed before and after a large air-gap magnet. The production muon will have very nearly the same direction as the primary neutrino for the coherent production. Schwartz exploits this fact to better establish the primary neutrino's direction. The "decay neutrino" from the $W^+ \rightarrow \mu^+ + \nu$ decay naturally escapes detection, thus leaving 4 unmeasured quantities, the primary neutrino energy and the three missing variables of the decay neutrino. Each coherent event is thus a "0-c event". He would then plot the calculated mass of the $\mu^+ + (\text{decay neutrino})$ system and would presumably see a narrow peak at the W mass. We shall return briefly to this point later in order to illustrate a possible difficulty with this technique.

B. Hadronic Decay Modes

The most systematic analysis of the semi-leptonic decay data is due to Cabibbo⁴. Figure 2a summarizes the hadronic currents allowable in his theory. The horizontal solid lines are the $\Delta S = 0$ currents whose strengths are proportional to $\cos \theta_c$. The 60-degree lines correspond to $\Delta S = \Delta Q$ currents and are proportional to $\sin \theta_c$.

Each solid line* of Fig. 2a suggests the hadronic decay mode,

$$W \rightarrow \bar{H}_{\mathbb{8}}(1/2^+) + H'_{\mathbb{8}}(1/2^+) \quad (3)$$

and in particular,

$$\underline{\Delta S = 0}: W^+ \rightarrow \bar{n} + p, \bar{\Sigma}^- + \Sigma^0(\Lambda), \Sigma^+ + \bar{\Sigma}^0(\bar{\Lambda}), \bar{\Xi}^- + \Xi^0 \quad (4)$$

$$\underline{\Delta S = \Delta Q}: W^+ \rightarrow \bar{\Sigma}^- + n, \bar{\Sigma}^0(\Lambda) + p, \bar{\Xi}^- + \Sigma^0(\Lambda), \bar{\Xi}^0 + \Sigma^+.$$

Here, H and H' are members of the same $J^P = 1/2^+$ SU(3) octet.

From Fig. 2b we infer the following 0^- mesonic decay modes.

$$\underline{\Delta S = 0}: W^+ \rightarrow \bar{K}^0 + K^+, \pi^+ + \pi^0(\eta) \quad (5)$$

$$\underline{\Delta S = \Delta Q}: W^+ \rightarrow \pi^+ + K^0, K^+ + \pi^0(\eta). \quad (6)$$

Similar inferences can be drawn from Fig. 2c which involves hadrons H and H' both of which are members of the $J^P = 3/2^+$ decimet. Figure 2d does the same for the octet of vector mesons.

H and H' need not be restricted to be members of the same SU(3) family. For example, it is now known that neutrino interactions of the form,

$$\nu + p \rightarrow \mu^- + \Delta^{++} \quad (7)$$

occur frequently, which implies that another class of decay modes exists

$$W \rightarrow \bar{H}_{\mathbb{8}} + H'_{\mathbb{10}}. \quad (8)$$

Some of the rarer leptonic decays of the K^+ such as $K^+ \rightarrow \pi^+ \pi^- e^+ \nu$ suggest decay modes

$$W \rightarrow \bar{H}_{\mathbb{8}}(0^-) + H'_{\mathbb{8}}(1^-), \quad (9)$$

and finally one should consider decays into more than two hadrons.

The point of all this is to emphasize that the W has a very large number of hadronic decay modes, none of which is likely to be dominant if the mass of the W is ≥ 5 BeV.

Regardless of the size of the leptonic decay rate, any single hadronic mode is likely to have a very small branching ratio. Any experiment should attempt to simultaneously detect as many of these, with as high a measurement precision as is

* The dashed lines correspond to $\Delta Q = 0$ or neutral lepton currents. Thus far, no non-electromagnetic neutral lepton currents have been detected.

possible. Unless the mass of the W is excessive (e.g., ≥ 30 BeV), the width of the W is likely to be narrower than the experimental resolution. Any improvement in the resolution function will result in a corresponding enhancement of the "signal-to-noise" ratio for that particular mass combination.

C. Particle Identification (Hadrons)

The two-body fragments will have momenta approximately equal to one-half the W mass. Considering this fact, the following classification of decay fragments is made to assist in understanding the identification problem. The letters in parentheses are the mean decay lengths in meters for 4 BeV/c momenta.

1. Particles that are unlikely to decay in the chamber
 - (a) Charged: $p(\infty)$, $\pi^\pm(223.0)$, $K^\pm(30.0)$
 - (b) Neutral: $n(\infty)$, $K_L^0(130.0)$, $\gamma(\infty)$
2. Particles that are likely to decay in the chamber*
 - (a) Charged: $\Sigma^\pm(0.082, 0.165)$, $\Xi^\pm(0.151)$, $\Omega^\pm(0.093)$
 - (b) Neutral: $K_S^0(0.208)$, $\Lambda(0.270)$, $\Xi^0(0.276)$
3. Conversion of non-decaying neutrals

Assuming that all particles that decay in the chamber will be identified, our main task is to place converting material at the appropriate location to make the non-decaying neutrals visible. If nothing is placed in their way, other than, say, liquid hydrogen, we are faced with the following facts:

1. Neutrons--The mean free path is 3.7 meters (if the n-p cross section is geometrical).
2. γ 's--The radiation length of liquid hydrogen is 10 meters.
3. K_L^0 's--Although the mean interaction length in liquid hydrogen is ~ 10 meters, one can infer the number of events with K_L^0 's from the K_S^0 's that decay in the chamber and can correct for their loss.

D. Production and Decay Characteristics of the W

If one assumes that the production process illustrated in Fig. 4b favors low momentum transfer to the H-H' system, one discovers from the kinematics that the W and l have the same velocity and carry most of the momentum of the incident neutrino. The W, being far more massive, gets most of it. This becomes truer the higher above threshold one goes. Even at threshold it is a good approximation. For simplicity we choose $M = M' = 1 \text{ BeV}/c^2$ as the mass of H and H'. Ignoring the muon mass, we obtain

*We do not include those particles that decay at the production vertex, such as Δ , K^{*0} , ρ , ω , ϕ , and η .

$$P_w^{th} = \frac{W^2}{2M} \left(1 + \frac{M}{M+W} \right) \tag{10}$$

with

$$E_{\nu th}^{lab} = \frac{(W+M)^2}{2M}. \tag{11}$$

For example, the lab momentum of an $8 \text{ BeV}/c^2$ W at threshold is $35 \text{ BeV}/c$ which is to be compared with the lab momentum of the incident neutrino of $40 \text{ BeV}/c$. Therefore, in order to simplify the remaining arguments, we shall assume that the W gets all the neutrino's energy and that the accompanying lepton has the same velocity as the W .*

Two important consequences follow from this simplification:

1. The hadronic decay fragments of the W are mostly thrown forward in the laboratory with typical decay angles of

$$\theta \approx \frac{M_w}{E_{\nu lab}}. \tag{12}$$

Figures 3a and 3b illustrate the decay ellipses for an $8 \text{ BeV}/c^2$ W into fragments whose rest masses are small compared with $M_w/2$.

2. The μ^+ or $\mu^-(e^-)$ will move relatively slowly in the laboratory. Even if one ignores the $1 - \gamma_5$ effect, the μ^- momentum will be only,

$$p_{\mu^-} \approx E_{\nu} \frac{m_{\mu}}{M_w} = 0.9 \text{ BeV}, \tag{13}$$

(for $M_w = 8 \text{ BeV}/c$ and $E_{\nu} = 70 \text{ BeV}$).

Here we would like to return to the Schwartz experiment that relied heavily upon the μ^- having the same direction as the incident neutrino. First, coulomb scattering in the U will be excessive. The range of a 1-BeV muon in U is ≈ 0.5 meters which is nearly the thickness of the target. If one now adds the effect of the $1 - \gamma_5$ terms, one finds the μ^- with much less than 1 BeV/c momentum in the laboratory.

A bubble chamber like the BNL 25-ft, surrounded with conversion material such as Ne-H mixture would seem to be a very useful detector that could readily detect these muons of momentum lower than 1 BeV. The trapping momentum for the 25-ft

*The dynamics of the $1 - \gamma_5$ interaction forces an energetic μ^- to be left-handed. In order to conserve helicity, the μ^- would prefer to be at rest or to move backward in the lab. The W^+ moves forward with -1 helicity. When the W^+ decays, the μ^+ decays backward in the W rest frame. This causes it to have low momentum in the laboratory.

chamber is ≈ 1.5 BeV. Many of these μ^- 's would stop and decay in the hydrogen part of the chamber.

Before we specify a particular configuration of the surrounding blanket of Ne-H mixture let us look briefly at the problems associated with making a reliable measurement of the total neutrino cross section.

III. TOTAL NEUTRINO CROSS SECTION AT HIGH ENERGIES

Bjorken⁵ has reviewed for us the phenomenon of the "deep inelastic" scattering of electrons on protons and has pointed out the possible similarities that might occur for neutrino-proton interactions. Figure 4 summarizes the neutrino analogue to the "deep inelastic" scattering of electrons.

A. Minimum Momentum Transfer Processes

Even though the mass M' might be large, at minimum momentum transfer the velocity of the recoiling hadron system of mass M' in the lab is not likely to be large. Therefore, the decay fragments of M' are likely to go in all directions in the laboratory.

B. Large Momentum Transfer

The most interesting of the inelastic processes are those involving very large momentum transfers to the hadron system. This system moves with substantial γ (~ 3) in the forward direction, casting its hadrons into the forward cone ($\theta \sim 1/3$ radians = 20°).

If a reliable estimate of the neutrino energy is to be made, we must try to convert as many of the non-decaying neutrals as possible. Because the neutrino energy spectrum may be rapidly falling in the region of interest, an error in the measurement of E_ν would give one a very wrong value of the ν flux and hence a wrong value of the cross section.

Considering the low-momentum-transfer events emitting fragments in all directions, and the very interesting large-momentum-transfer events throwing fragments in the forward cone, we would wish to place converting material both downstream and at right angles.

IV. THE 25-FT BNL CHAMBER AS A DETECTOR

When the whole chamber is filled with neon, the neutral conversion problem is automatically solved. When H_2 and D_2 are to be used as target materials, one would employ the new techniques of using a surrounding blanket of Ne- H_2 mixture to act as the converting material. The dashed curves of Fig. 5a illustrate a number of different possible arrangements. One of these is to place in the chamber a cylinder with a flat end, another would place a dome on the end of the cylinder.

Since the physics indicates two classes of processes, those emitting neutrals transversely and those emitting them longitudinally, separate calculations have been

made for transverse detection efficiency of neutrals and for longitudinal efficiency. Figure 6a summarizes the transverse efficiency multiplied by the volume of the cylinder as a function of the radius of a cylinder 4.8 meters long. A 30% atomic composition⁶ of neon was assumed with a γ conversion length of 0.70 m and a neutron conversion length of 2.5 m. Conversion in the H_2 or D_2 is not taken into account. These curves give the effective volume for doing $1\pi^0$, $2\pi^0$, $3\pi^0$, and 1-neutron physics where these particles are emitted at right angles to the neutrino beam. Figure 6b displays similar curves for the longitudinally emitted neutrals* as a function of the length of the cylinder. Figure 6c is the same display but for a cylinder with a dome on the end. Both Figs. 6b and 6c are done for a 1-meter radius cylinder. If a larger cylinder is chosen these values will increase as the square of the radius. Figures 6d, 6e, and 6f, respectively, give the detection efficiencies.

We shall defer the discussion of the optimum shape of the cylindrical insert until we hear of the low-energy neutrino physics requirements and of the strong interaction requirements.

V. ENLARGED 25-FT BNL CHAMBER AS A DETECTOR

Palmer⁷ has suggested making the 25-ft BNL chamber spherical in shape (radius = 3.43 meters) keeping the coils and the vacuum chamber fixed. For a modest fractional increase in cost one obtains nearly a factor of four increase in the effective volume.** Figure 7a shows the effective volume of a domed cylindrical insert as a function of its radius. Figure 7b gives detection efficiencies. Here the dome is concentric with the full chamber radius. A comparison of Fig. 7a with Fig. 6a demonstrates the factor of four increase. In this configuration, the downstream neutrals are given slightly more advantage than the transverse neutrals. If much more advantage should be given to downstream neutrals then the center of the dome could be shifted upstream and the calculation repeated for both transverse and longitudinal neutrals.

Another possibility would be to make the insert spherical with its center shifted upstream. The broken line of Fig. 7a gives the volume of the spherical insert.

*The most troublesome experimental problem for forward moving hadron systems is the missing neutron that is likely to carry a substantial portion of the momentum. For the neutron the volume is the least.

**The effective volume is defined as the volume of the inscribed domed cylinder multiplied by the probability of one- π^0 , two- π^0 , three- π^0 , or one-neutron conversion.

VI. TRACK SENSITIVE TARGETS PLACED IN THE 12-FT ARGONNE CHAMBER

The upper part of Fig. 8b shows a possible H_2 or D_2 insert that could be placed in the 12-ft Argonne chamber. Figure 8a displays the approximate* effective volume of the chamber for doing physics in which the neutrals are thrown into the forward cone of half angle of ~ 60 degrees. Figure 8b gives the corresponding detection efficiencies.

VII. THE IMPORTANCE OF HIGH MAGNETIC FIELD

A. Curvature

G. Ascoli⁸ and P. Slattery⁹ have emphasized that for strong-interaction physics in the 25-ft BNL chamber the high magnetic field (40 kG) plays a secondary role to the angle accuracy in determining missing mass values. In their view not much would be lost by reducing the field to 30 kG.

For much of the high-energy neutrino physics the roles of magnetic field and angles are reversed. For neutrino physics, the neutrino's energy, one of the most important variables is unmeasured. For hadron physics the incident particle momentum can be measured to high precision. For those neutrino events that convert all their neutrals, the neutrino energy is determined by summing the measured energy of all outgoing particles and subtracting the target mass. For high-momentum particles, the error in this sum depends directly on the error of the curvature measurement which in turn depends upon the magnetic field. Nothing needs to be known about their direction. The angles are, however, important in deciding whether the event has converted all its neutrals. It is highly desirable to reduce the fraction of events with neutrals that completely escape detection. For this, one needs a large chamber (perhaps even larger than the 25-ft BNL chamber). In order to reduce this fraction even further there will be motivation to use pure neon as the surrounding blanket of converting material rather than a 30%-neon H_2 mixture. Coulomb scattering will then be greater, thereby requiring even higher field in order to maintain accuracy. Under these conditions in order to measure high-energy γ -ray energies, one will use the techniques of measuring the whole shower energy. Again we feel the high magnetic field will make this more reliable.

For the hadronic decay modes of the W, where one measures all its decay fragments in order to measure its invariant mass, the arguments of Ascoli and Slattery would apply.

*We have assumed that neutrals emitted sideways through the ends of the cylinder leave the same efficiency for conversion as those emitted at 45° through the cylindrical wall. This overestimates the effective volume.

B. Trapping

There are other reasons for the high field. Trapping of particles in order that they may identify themselves will aid in the ambiguity problem. The higher the field the more will be trapped. We have already referred to the leptonic decay of the W^+ as indicating a need for trapping the ≈ 1 GeV/c production μ^- and perhaps the decay μ^+ as well.

REFERENCES

- ¹D. Frisch, Beam and Spark-Chamber Detector for Search for W's Produced by Neutrinos, National Accelerator Laboratory 1968 Summer Study Report B. 1-68-66, Vol. I, p. 235.
- ²A. K. Mann, W Searches with High Energy Neutrinos and High Z Detectors, National Accelerator Laboratory 1969 Summer Study Report SS-16, Vol. IV.
- ³Mel Schwartz, Proposal at an informal meeting of potential spark-chamber users at NAL, Batavia, Illinois, April 1, 1968 (unpublished).
- ⁴N. Cabibbo, Phys. Rev. Letters 10, 531 (1963).
- ⁵Bjorken, 1969 Summer Study Lectures.
- ⁶25-Foot Cryogenic Bubble Chamber Proposal.
- ⁷R. B. Palmer et al., Reconsideration of a Spherical 25-Foot Bubble Chamber in the Light of Sensitive Targets, National Accelerator Laboratory 1969 Summer Study Report SS-82, Vol. II.
- ⁸G. Ascoli, Choice of Magnetic Field for the 25-Ft Chamber, National Accelerator Laboratory 1969 Summer Study Report SS-103, Vol. II.
- ⁹P. Slattery, (unpublished).

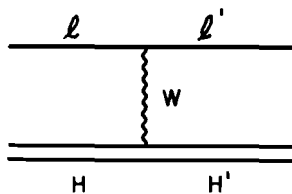


Fig. 1(a). Role of the W-meson in semi-leptonic decay.

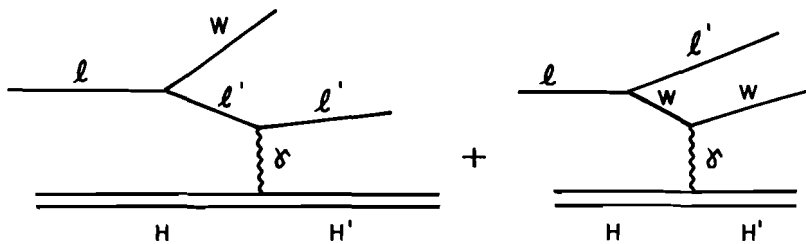


Fig. 1(b). Possible production modes of the W-meson.

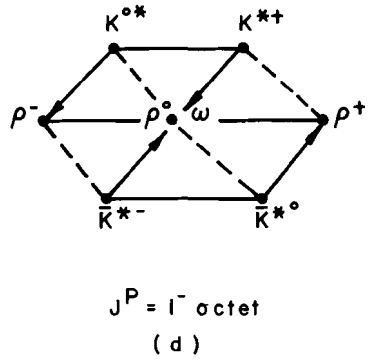
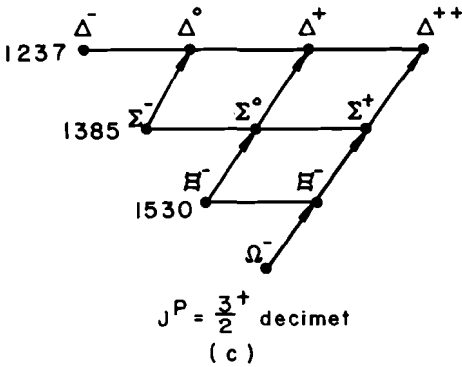
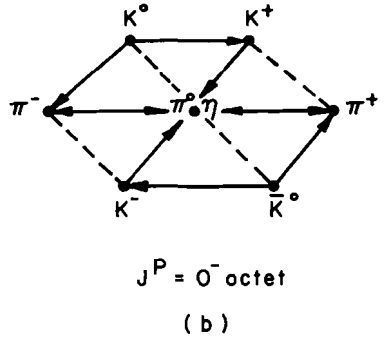
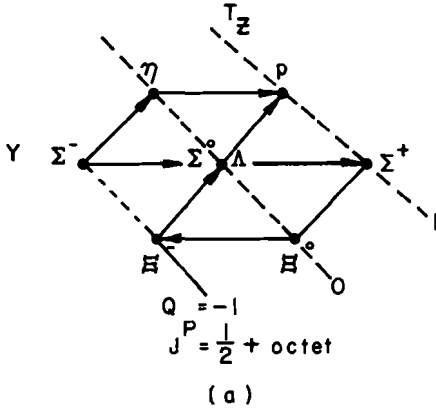
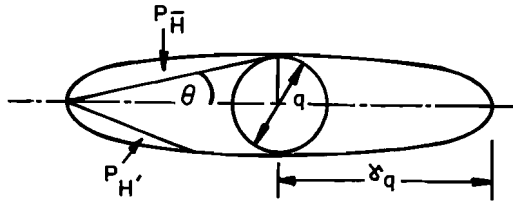
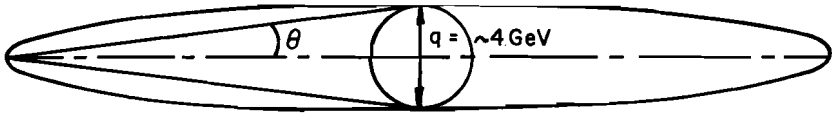


Fig. 2 (a) Hadronic currents allowed in the Cabibbo theory are indicated by arrows. (b) Allowed currents in the pseudoscalar octet. (c) Currents in the $3/2^+$ decimet (d) Currents in the vector octet.



(a)



(b)

Fig. 3. Decay ellipses for an $8 \text{ BeV}/c^2$ W into fragments whose rest masses are small compared with $M_W/2$.

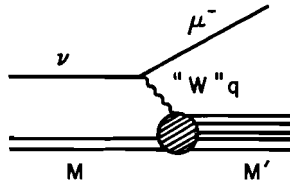


Fig. 4. Neutrino analogue of deep inelastic scattering of muons.

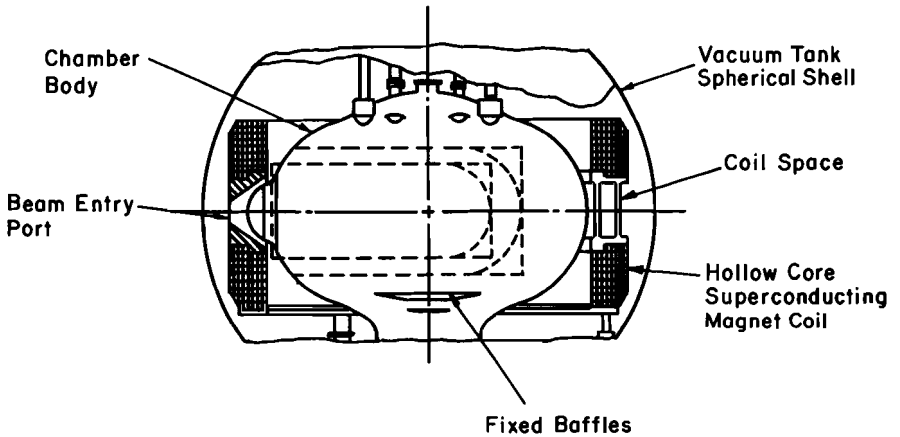


Fig. 5. The dotted lines illustrate possible arrangements of internal track-sensitive hydrogen targets inside a Ne-H mixture.

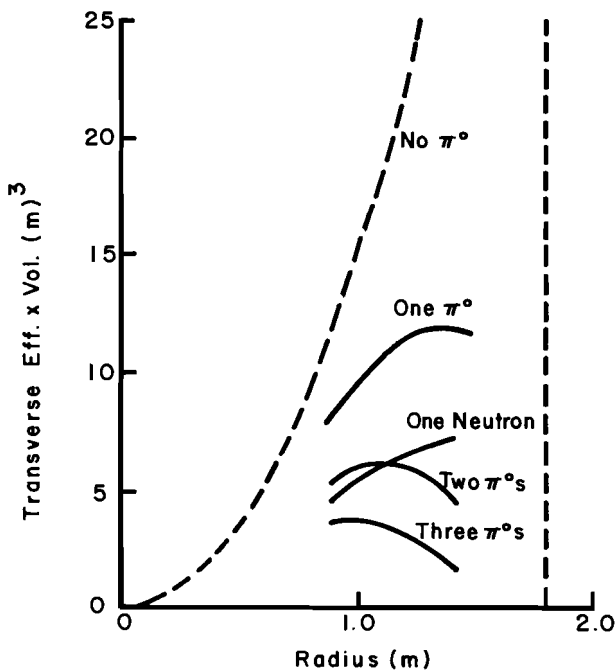


Fig. 6(a). Neutral detection transverse efficiency \times volume as a function of radius of a cylinder 4.8 meters long.

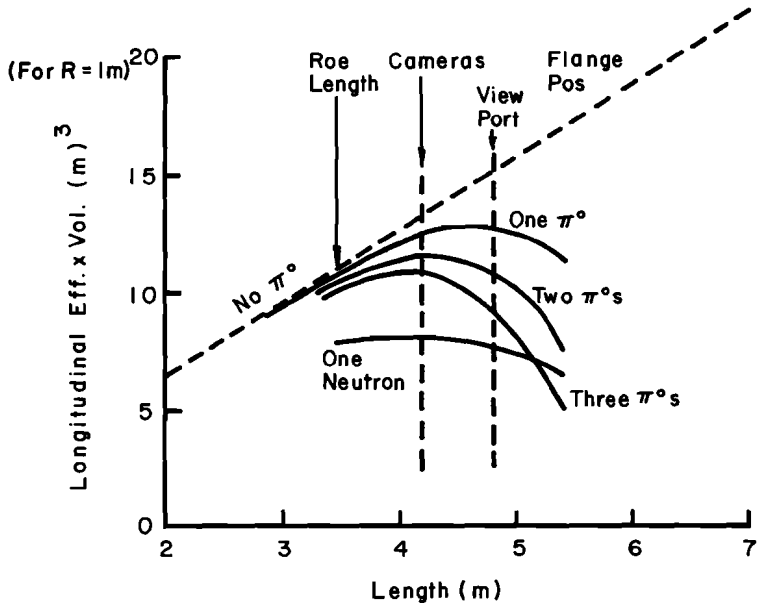


Fig. 6(b). Neutral detection longitudinal efficiency \times volume as a function of cylinder length.

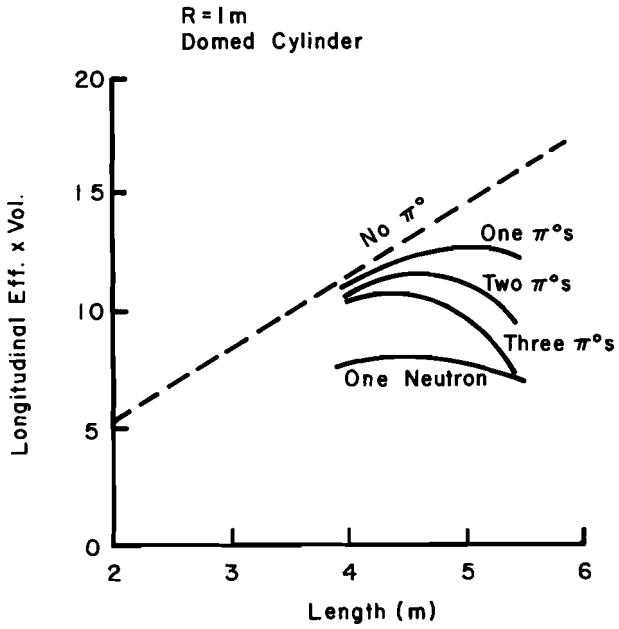


Fig. 6(c). Neutral detection longitudinal efficiency \times volume as a function of cylinder with dome on one end.

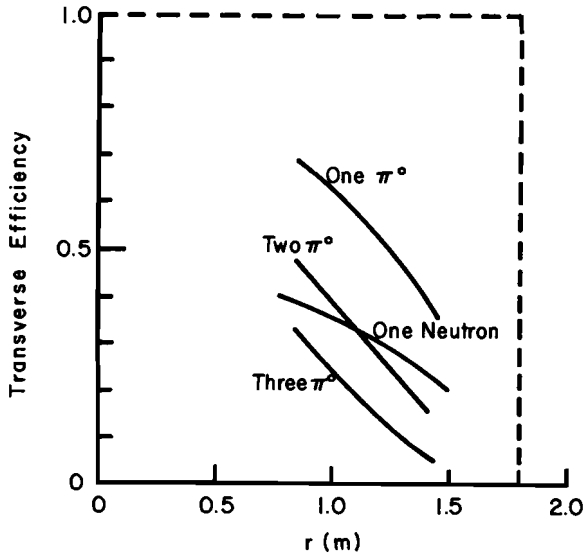


Fig. 6(d). Efficiency for transverse neutrals, case described in Fig. 6(a).

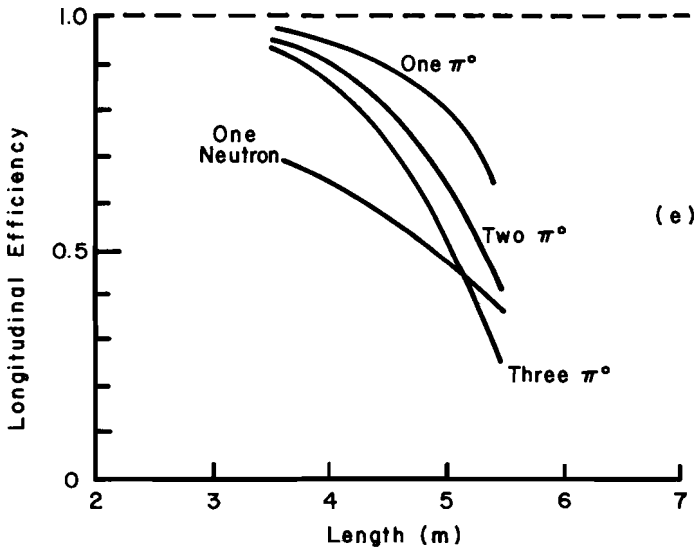


Fig. 6(e). The efficiency for the longitudinal case, Fig. 6(b).

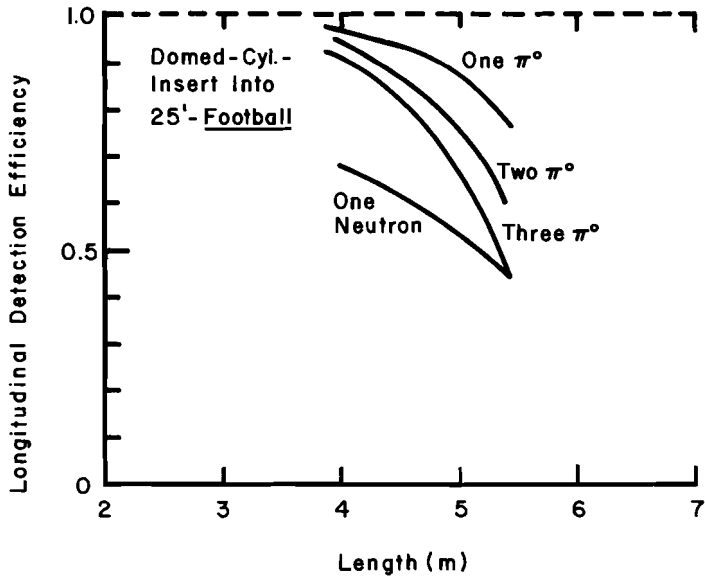


Fig. 6(f). Detection efficiency for case described in Fig. 6(c).

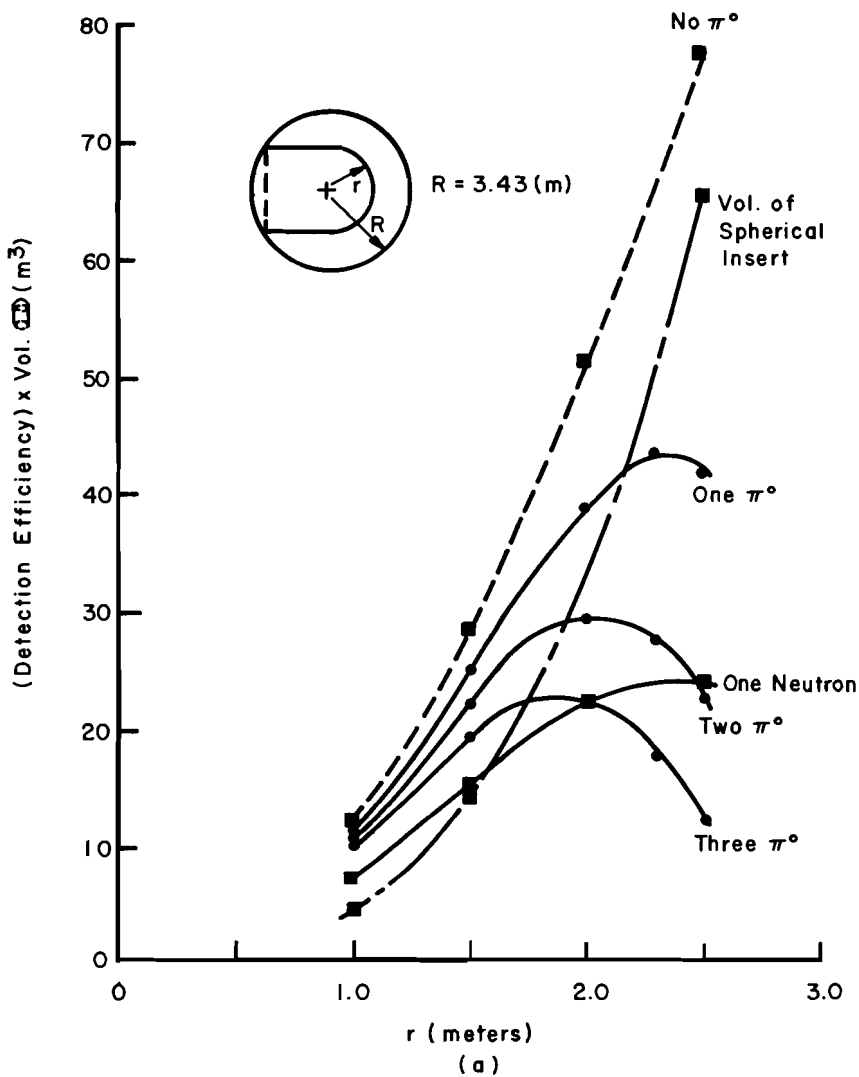


Fig. 7(a). Detection efficiency \times volume for a domed cylinder.

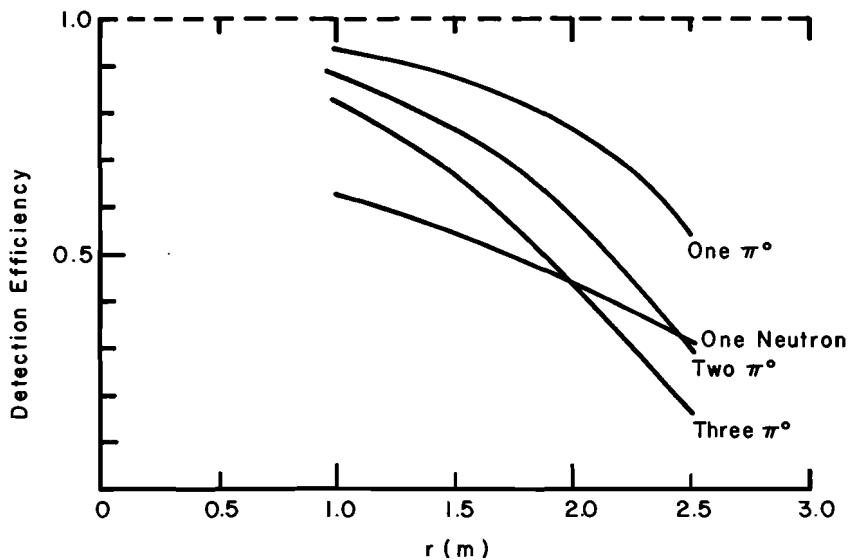


Fig. 7(b). Detection efficiency for a domed cylinder.

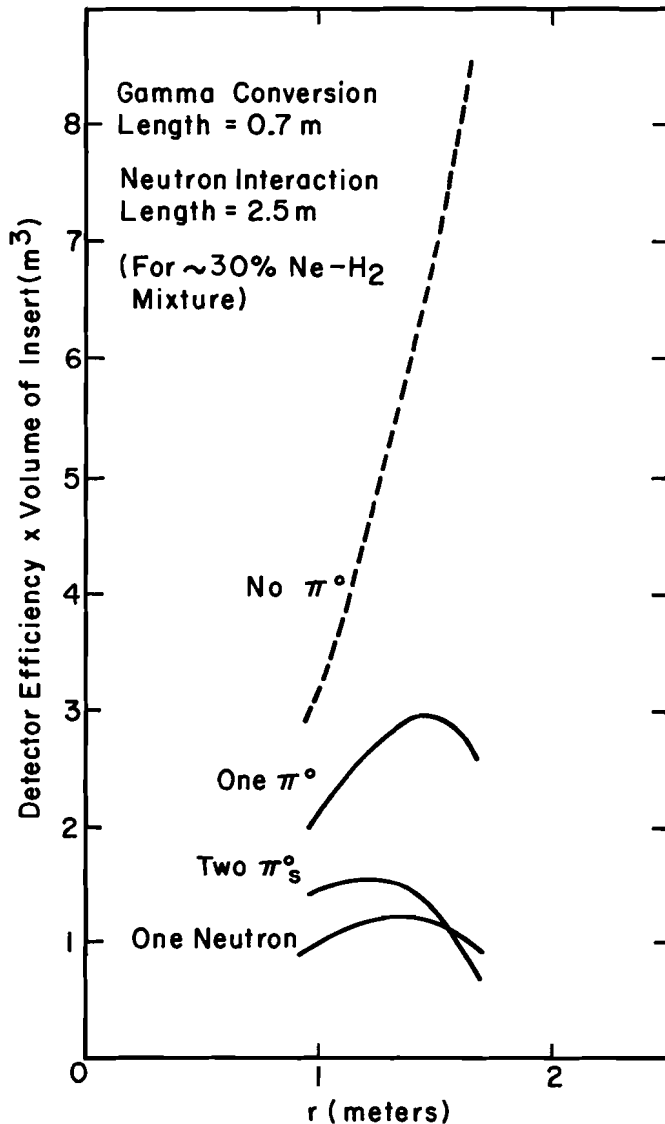


Fig. 8(a). Effective volume for a conversion of the Argonne 12-ft chamber. Gamma conversion length 0.7 m, neutron interaction length 2.5 m. See insert in Fig. 8(b) for geometry.

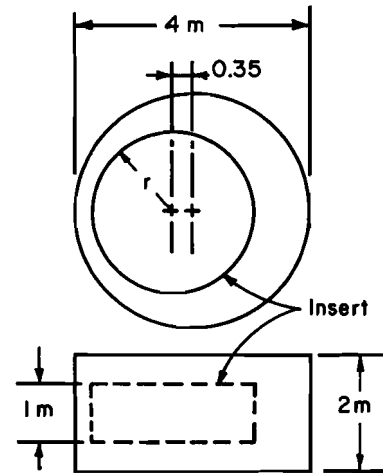
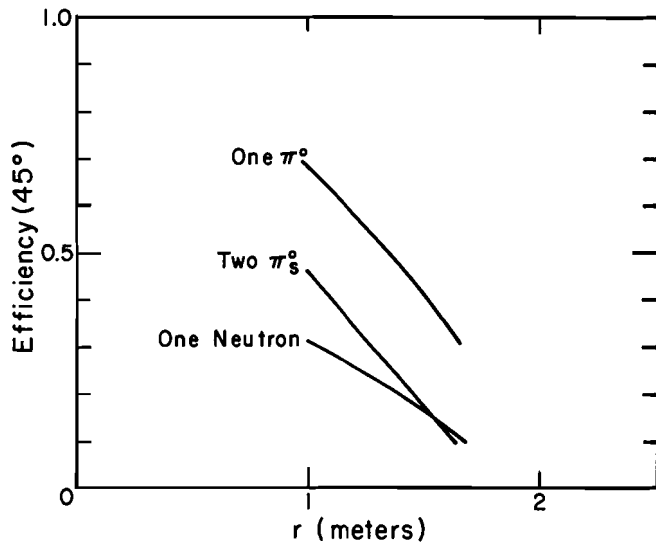


Fig. 8(b). Detection efficiency of system of Fig. 8(a).